Microwave-assisted synthesis of novel sulfonamide-based compounds bearing α-aminophosphonate and their antimicrobial properties

Eman Sabry [a,*], Hanan A. Mohamed [b], Ewies F. Ewies [c], Benson M. Kariuki [d], Osama M. Darwesh [e], Mohamed S. Bekheit [a]

[a] *Department of Pesticide Chemistry, National Research Centre, Dokki, Giza 12622, Egypt*
[b] *Applied Organic Chemistry Department Chemical Industries Research Institute, National Research Centre, Dokki, Giza 12622, Egypt*
[c] *Organometallic and Organometalloid Chemistry Department, National Research Centre, Dokki, Giza 12622, Egypt*
[d] *School of Chemistry, Cardiff University, Main Building, Park Place, Cardiff, CF10 3AT, UK*
[e] *Agricultural Microbiology Department, National Research Centre, Dokki, Giza 12622, Egypt*

a r t i c l e i n f o

Keywords:
α-aminophosphonate
Sulfisoxazole
Antimicrobial
Microwave-assisted
One-pot reaction
Molecular modeling

a b s t r a c t

A series of α-aminophosphonates (**3a-3m**) bearing the sulfisoxazole moiety was synthesized through one-pot Kabachnik-Fields reaction of sulfisoxazole, diethyl phosphite (DEP) and substituted aldehydes using bismuth (III) triflate [Bi(OTf)$_3$] as a catalyst under microwave reaction conditions. The novel compounds are identified by their spectroscopic data and confirmed by X-ray diffraction studies of diethyl (4-chlorophenyl)(4-(N-(3,4-dimethylisoxazol-5-yl)sulfamoyl)phenylamino) methylphosphonate **3g**. The antimicrobial properties of the synthesised agents were examined against a range of bacterial species and *C. albicans* yeast. Some of the synthesised agents, **3j, 3l** and **3m,** exhibit potent antimicrobial activ-ities against the five pathogenic microorganisms used in the investigation. Compound **3m** is the most promising agents among all the synthesized derivatives, showing a potent and broad-spectrum antibac-terial activity. The MIC values are 94.2 and 205.7 μM for **3m** and sulfisoxazole, respectively for *S. typhi* (about 2.1 times potency). The MIC values are 102.8 and 187.0 μM for **3m** and sulfisoxazole, respectively for *L. monocytogenes*. The observed biological properties are explained and supported by QSAR models.

1. Introduction

In recent decades, numerous cases of drug-resistance in human pathogenic microorganisms have been recorded. Inaccurate diag-nosis and widespread misuse of antibiotic agents have been pri-mary causes for the increase in multidrug resistance [1,2]. A re-port by the World Health Organization (WHO) has forecast that antimicrobial resistance will contribute to 10 million deaths an-nually by 2050. In addition, it will force 24 million people into extreme poverty by 2030 [3]. Among these drug-resistant mi-crobes are methicillin resistant *S. aureus* (MRSA) and vancomycin-resistant *Enterococci* (VRE) [4]. Treatment of these infections by such pathogens is a major hurdle, particularly in immunocompro-mised patients [5]. New powerful antimicrobial agents are there-fore needed to overcome this challenge. The main strategies for accomplishing this aim is the discovery of new antimicrobial phar-macophores and/or the modification of known antimicrobial agents [6,7]. Molecular hybridization is a novel approach in drug develop-ment that aims to create a new hybrid molecule with better affin-ity by combining two potent pharmacophores [8].

Sulfonamides are synthetic bacteriostatic drugs which block the bio-synthetic pathway of folic acid (bacteria growth inhibitor). Sul-fonamides are used as antibiotic agents with wide-spectrum ac-tivities against a panel of bacterial species, most of them Gram-positive and many Gram-negative. However, many strains of an in-dividual species may be resistant [9]. Sulfonamides also exhibit sig-nificant biological activities such as carbonic anhydrase inhibitor [10], antiviral [11], anti-inflammatory [12], anticancer [13], and an-tifungal agents [14].

Sulfisoxazole is sulphonamide antibiotic with a dimethyl isoxa-zole substituent that has a broad spectrum and a short duration of action with activity against Gram-negative and Gram-positive organisms. Sulfisoxazole is used in combination with other an-tibiotics to treat and prevent bacterial infections [15]. Sulfisoxa-zole prevents bacteria multiplication by acting as a competitive inhibitor to *p*-amino benzoic acid (pABA) substrate for the active site of the dihydropteroate synthase enzyme (DHPS) and thus in-hibits dihydrofolic acid generation. DHPS supports the biosynthe-

* Corresponding author.
E-mail address: eman_sabry2021@yahoo.com (E. Sabry).

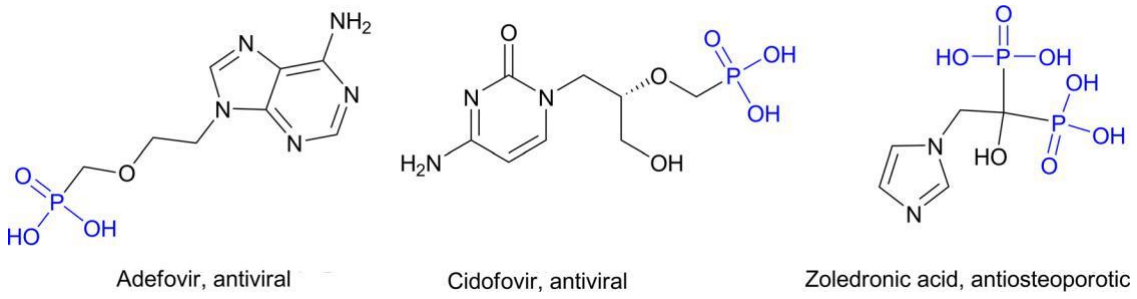

Fig. 1. Examples of some phosphonate compounds currently in medicinal use.

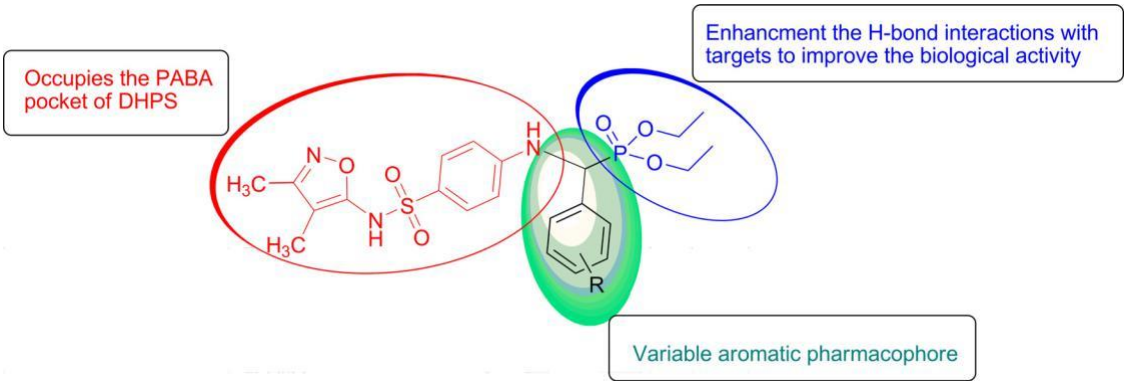

Fig. 2. Structure of the target α-aminophosphonates.

sis of the folic acid intermediate from pABA and dihydropterin-6-hydroxymethyl pyrophosphate (DHPP) [15].

Phosphonate compounds considered as a bioisosteres of car-boxylates and as analogs of carboxylic acids, amino acids and peptides. Phosphonates are characterized by their bioactive prop-erties and so have found application as drugs or pro-drugs

[16] (Fig. 1). Among the potent phosphonate compounds are α-aminophosphonic acids (APAs) and their ester derivatives. They have attracted the attention of many scientific researchers because they have pivotal medicinal roles as peptide mimics, herbicides, pharmacological agents and many other applications [17–20]. α-

Aminophosphonates are characterized by high metabolic stabil-ity, biological efficiency, and minimal toxicity in mammalian cells

[21]. They are particularly essential as antimetabolites because of their low mammalian toxicity and their ability to mimic aminocar-boxylic acids. They compete with their carboxylic counterparts for the active sites of enzymes and cell receptors [22,23]. For example, addition of an aminophosphonate group to a pharmacophore core can boost the antitumor activity [24,25]. Many aminophosphonate compounds have been demonstrated to be effective inhibitors of human cancer cells [26–28]. α-Aminophosphonate derivatives have been reported do display enzyme inhibitor [29,30], antimicrobial [31], antiviral [32], anti-Alzheimer's [33] and antibacterial activity

[34].

Several protocols have been documented for the synthesis of α-aminophosphonate derivatives, including the traditional Lewis acid-catalysed addition of di-/trialkyl phosphite to imine (Pudovik reaction) [35]. An alternative method for α-aminophosphonate synthesis is the Kabachnik-Fields (Phospha-Mannich condesation) reaction. The Kabachnik-Fields reaction involves the one-pot reac-tion of dialkyl phosphite, oxo compounds (aldehydes or ketones) and primary or secondary amines in the presence of efficient acidic or basic catalysts [36,37]. Lewis and Brønsted acid catalysts play a critical role in many organic synthesis reactions that are character-ized by high selectivity, stability in the reaction medium and so are highly amenable to recyclability, including metal triflates [38–40].

The Kabachnik-Fields reaction has a drawback in that the water generated can deactivate or decompose the catalyst. Metal triflates are water tolerant and so they are suitable for the Kabachnik-Fields condensation reaction [41].

An important aspect of green chemistry is the generation of chemical products by decreasing or eliminating environmentally hazardous compounds [42]. Multi-component reactions are an ex-ample of eco-friendly reaction which are characterized by high yields, atom-/step economy and reduced reaction time [43,44]. Microwave (MW) radiation has gained prominence as an energy source in organic synthesis. It has several advantages over conven-tional heating in addition to acceleration of the reaction rate. These include high yields, minimal side-products, high selectivity as well as ease of purification and isolation of the products [45]. The use of microwave conditions for the generation of α-aminophosphonates *via* the Kabachnik-Fields reaction has been reported and reviewed [37,46,47].

In line with the foregoing considerations and as part of our pre-vious and on-going studies [48–52], we have designed a new se-ries of α–aminophosphonates tagged with sulfisoxazole *via* MWI-assisted Kabachnik–Fields reaction. The synthesized compounds were thereafter tested *in vitro* for their antimicrobial activities (Fig. 2).

2. Materials and Methods

2.1. Experimental

Melting points were determined with an open capillary tube on an Electrothermal (variable heater) melting point apparatus and are uncorrected. IR spectra (KBr) were recorded on a Shimadzu FT-IR 8400S spectrophotometer. Reactions were monitored using thin layer chromatography (TLC) on 0.2 mm silica gel F254 plates (Merck) utilizing various solvents for elution. The chemical struc-tures of the synthesized compounds were characterized by nuclear magnetic resonance spectra (^{1}H NMR, ^{13}C NMR) recorded on a

JEOL NMR spectrometer (500 MHz, 125 MHz for ^{1}H and ^{13}C, respectively). Chemical shifts are reported in parts per million (ppm) using the deuterated solvent peak as an internal standard.

The purity of all new samples was verified by microchemical analysis (C/H/N) carried out at the Microanalysis Laboratory, Cairo University, Cairo, Egypt. The microwave oven used is a Milestone Italy (model: StartSynth, Reactor: Pack2B Basic Single Vessel Kit).

2.1.1. Synthesis

General procedure for the synthesis of α-aminophosphonates 3a-3m. A solution of equimolar amounts of the sulfisoxazole (**1a**) (0.5 g – 1.87 mmol) in absolute ethanol (10 ml) was placed with a mag-netic stirring bar a microwave quartz vessel. Diethyl phosphite (0.26 g, 1.9 mmol) and substituted benzaldehyde (1.87 mmol) (**2a-2m**) were added, followed by the addition of (10 mol%) $Bi(OTf)_3$. The reaction mixture was heated in the microwave reactor at 60 °C for the appropriate time (40–60 min) at 60 Watt. After com-pletion of the reaction (TLC), the product mixture was allowed to cool down, concentrate, and the residue was dissolved in ethyl acetate (50 mL), and washed with water (3 × 50 mL). The or-ganic phase was dried over anhydrous sodium sulfate and subse-quently filtered and concentrated to afford the corresponding α-aminophosphonate products **3a-3m** and recrystallized from a suit-able solvent.

Diethyl (4-(N-(3,4-dimethylisoxazol-5-yl)sulfamoyl)-phenylamino)(phenyl) methyl phosphonate (**3a**) was obtained as a greenish solid (0.81 g, 88%); mp 210-212°C (EtOH); ^{1}H NMR (500 MHz, DMSO): δ =1.00 (t, 3H, *H3*CCOP), 1.12 (t, 3H, *H3*CCOP), 1.50 (s, 3H, *H3*C), 1.99 (s, 3H, *H3*C), 3.66- 3.71 (m, 1H, *H*C-OP), 3.83- 3.87 (m, 1H, *H*C-OP), 3.97-4.02 (m, 2H, *H2*C-OP), 5.17 (dd, 1H, *J* = 9.6 & 23.8 Hz, *H*C-P), 6.89 (d, 2H, *J* = 8.6 Hz, H-Ar), 7.23 (d, 1H, H-Ar), 7.29-7.33 (m, 4H, H-Ar), 7.40 (t, 1H, N*H*), 7.49 (d, 2H, *J* = 7.65, H-Ar), 10.52 (s, 1H, N*H*-CP); ^{13}C NMR (125.7 MHz, DMSO): δ = 161.7, 156.9, 151.9, 151.8, 136.5, 128.8, 128.6, 128.1, 127.5, 126.9 113.1, 104.7 (*C*-Ar), 63.1, 63.0, 62.97, 62.93 (2O*C*H_2), 53.9 (d, $^{1}J_{PC}$ = 150.6 Hz, *C*-P), 16.8, 16.7, 16.57, 16.53 (2OC-*C*H_3), 10.8, 6.2 (2*C*H_3); IR (KBr): 3440 (2NH), 1388 (SO_2, asy), 1241 (P=O), 1137 (SO_2, sym), 1025 (2P-O-C) cm^{-1}; Anal. calcd. for $C_{22}H_{28}N_3O_6PS$ (493.51): C, 53.54; H, 5.72; N, 8.51. Found: C, 53.38; H, 5.91; N, 8.34.

Diethyl (4-(N-(3,4-dimethylisoxazol-5-yl)sulfamoyl)-phenylamino)(p-tolyl)methyl phosphonate (**3b**) was obtained as a white solid (0.74 g, 87%); mp 206-208°C (EtOH); ^{1}H NMR (500 MHz, DMSO): δ =1.04 (t, 3H, *H3*CCOP), 1.15 (t, 3H, *H3*CCOP), 1.50 (s, 3H, *H3*C), 2.01 (s, 3H, *H3*C), 2.22 (s, 3H, *H3*C), 3.67- 3.74 (m, 1H, *H*C-OP), 3.83- 3.89 (m, 1H, *H*C-OP), 3.97-4.03 (m, 2H, *H2*C-OP), 5.12 (d, 1H, *J* = 9.6 & 23.8 Hz, *H*C-P), 6.89 (d, 2H, *J* = 8.6 Hz, H-Ar), 7.11 (d, 2H, H-Ar), 7.34-7.39 (m, 5H, 4H-Ar+N*H*), 10.53 (s, 1H, N*H*-CP); ^{13}C NMR (125.7 MHz, DMSO): δ = 161.7, 156.6, 152.1, 152.0, 137.3, 133.4, 129.2, 128.6, 126.6, 113.1, 104.8 (C-Ar), 63.07, 63.01, 62.9, 62.8 (2O*C*H_2), 53.6 (d, $^{1}J_{PC}$ = 151.4 Hz, *C*-P), 21.2 (*C*H_3), 16.8, 16.7, 16.6, 16.5(2OC-*C*H_3) 10.7, 6.2 (2*C*H_3); Anal. calcd. for $C_{23}H_{30}N_3O_6PS$ (507.54): C, 54.43; H, 5.96; N, 8.28. Found: C, 54.62; H, 5.76; N, 8.13.

Diethyl (4-(N-(3,4-dimethylisoxazol-5-yl)sulfamoyl)-phenylamino)(4-methoxyphenyl) methylphosphonate (**3c**) was obtained as a yellow solid (0.98 g, 89%); mp 216-218°C (EtOH); ^{1}H NMR (500 MHz, DMSO): δ =1.02 (t, 3H, *H3*CCOP), 1.13 (t, 3H, *H3*CCOP), 1.50 (s, 3H, *H3*C), 2.00 (s, 3H, *H3*C), 3.66-3.72 (m, 4H, *H*C-OP + OCH_3), 3.83- 3.86 (m, 1H, *H*C-OP), 3.97-4.02 (m, 2H, *H2*C-OP), 5.09 (dd, 1H, *J* = 9.5 & 13.3 Hz, *H*C-P), 6.86-6.89 (m, 4H, H-Ar), 7.30-7.33 (m, 3H, H-Ar + N*H* exchangeable), 7.41 (d, 2H, *J* = 6.7, H-Ar), 10.51 (s, 1H, N*H*-CP- exchangeable); ^{13}C NMR (125.7 MHz, DMSO): δ = 161.7, 159.2, 156.6, 152.09, 152.0,130.0, 129.9, 128.6, 128.2, 126.5, 114.0, 113.1, 104.8 (C-Ar), 63.0, 62.96, 62.91, 62.8 (2O*C*H_2), 55.5 (O*C*H_3), 53.2 (d, $^{1}J_{PC}$ = 152.6 Hz, *C*-P), 16.8, 16.7, 16.6, 16.5 (2OC-*C*H_3), 10.7, 6.2 (2*C*H_3); Anal. calcd. for $C_{23}H_{30}N_3O_7PS$ (523.54): C, 52.77; H, 5.78; N, 8.03. Found: C, 52.58; H, 5.98; N, 7.86.

Diethyl (4-(N-(3,4-dimethylisoxazol-5-yl)sulfamoyl)-phenylamino)(4-hydroxyphenyl) methylphosphonate (3d) was obtained as a white solid (0.93g, 89%); mp 220-222°C (EtOH); ^{1}H NMR (500 MHz, DMSO): δ =1.01 (t, 3 H, *H3*CCOP), 1.12 (t, 3 H, *H3*CCOP), 1.50 (s, 3H, *H3*C), 2.00 (s, 3H, *H3*C), 3.64- 3.70 (m, 1H, *H*C-OP), 3.83- 3.85 (m, 1H, *H*C-OP), 3.94-4.00 (m, 2H, *H2*C-OP), 5.00 (dd, 1H, *J* = 9.5 & 23.9 Hz, *H*C-P), 6.68 (d, 2H, *J* = 8.6 Hz, H-Ar), 6.86 (d, 2H, *J* = 8.6, H-Ar), 7.22-7.34 (m, 6H, 4H-Ar & O*H* & N*H*), 9.1 (s, 1H, N*H*-CP); ^{13}C NMR (125.7 MHz, DMSO): δ = 161.6, 157.4, 156.7, 152.0, 151.9, 130.0, 129.9, 128.6, 126.6, 126.3, 115.4, 113.0, 104.6 (*C*-Ar), 62.94, 62.92 (2O*C*H_2), 53.3 (d, $^{1}J_{PC}$ = 152.6 Hz, *C*-P), 16.8, 16.7, 16.6, 16.5 (2OC-*C*H_3), 10.7, 6.2 (2*C*H_3); Anal. calcd. for $C_{22}H_{28}N_3O_7PS$ (509.51): C, 51.86; H, 5.54; N, 8.25. Found: C, 51.69; H, 6.47; N, 8.06.

Diethyl (4-(dimethylamino)phenyl)(4-(N-(3,4-dimethylis-oxazol-5-yl)sulfamoyl) phenylamino)methylphosphonate (**3e**) was obtained as a buff solid (0.85 g, 85%); mp 205-207°C (EtOH); ^{1}H NMR (500 MHz, DMSO): δ =1.02 (t, 3H, *H3*CCH2OP), 1.13 (t, 3H, *H3*CCH2OP), 1.49 (s, 3H, *H3*C), 2.00 (s, 3H, *H3*C), 2.82 (s, 6H, (*H3*C)2-N), 3.66- 3.71 (m, 1H, *H*C-OP), 3.83- 3.87 (m, 1H, *H*C-OP), 3.97-4.00 (m, 2H, *H2*C-OP), 4.95 (dd, 1H, *J* = 9.6 & 13.3 Hz, *H*C-P),
6.63 (d, 2H, *J* = 8.6, H-Ar), 6.86 (d, 2H, *J* = 8.6, H-Ar), 7.22-7.32 (m, 5H, 4H-Ar + N*H*), 10.52 (br, 1H, N*H*-CP); ^{13}C NMR (125.7 MHz, DMSO): δ = 161.7, 156.6, 152.2, 152.1, 150.3, 129.5, 129.4, 129.2, 128.6, 126.3, 123.1, 113.19, 113.11, 112.4, 104.8 (*C*-Ar), 62.85, 62.84, 62.81, 62.79(2O*C*H_2), 53.2 (d, $^{1}J_{PC}$ = 153.8 Hz, *C*-P), 39.5 ($N(CH_3)_2$), 16.85, 16.81, 16.68, 16.64 (2OC*C*H_3), 10.7, 6.3 (2*C*H_3); Anal. calcd. for $C_{24}H_{33}N_4O_6PS$ (536.58): C, 53.72; H, 6.20; N, 10.44. Found: C, 53.51; H, 6.37; N, 10.25.

Diethyl (4-(N-(3,4-dimethylisoxazol-5-yl)sulfamoyl)-phenylamino)(4-fluorophenyl) methylphosphonate (**3f**) was obtained as a white solid (0.85 g, 89%); mp 215-217°C (EtOH); ^{1}H NMR (500 MHz, DMSO): δ =1.07 (t, 3H, *H3*CCH2OP), 1.14 (t, 3H, *H3*CCH2OP), 1.49 (s, 3H, *H3*C), 2.00 (s, 3H, *H3*C), 3.80- 4.06 (m, 4H, 2*H2*C-OP), 5.49 (dd, 1H, *J* = 9.5 & 24.8 Hz, *H*C-P), 6.55-6.62 (m, 1H, H-Ar), 6.91 (m, 2H, H-Ar), 7.33-7.37 (m, 2H, H-Ar), 7.79-7.82 (d, 2H, H-Ar), 10.55 (s, 1H, N*H*-CP); Anal. calcd. for $C_{22}H_{27}FN_3O_6PS$ (511.50): C, 51.66; H, 5.32; N, 8.22. Found: C, 51.48; H, 6.57; N, 12.39.

Diethyl (4-chlorophenyl)(4-(*N*-(3,4-dimethylisoxazol-5-yl) sulfamoyl)phenylamino) methylphosphonate (**3g**) was obtained as white crystals (0.83 g, 85 %); mp 202-204°C (EtOH); ^{1}H NMR (500 MHz, DMSO): δ = 1.04 (t, 3H, *H3*CCOP), 1.13 (t, 3H, *H3*CCOP), 1.47 (s, 3H, *H3*C), 2.00 (s, 3H, *H3*C), 3.73- 3.78 (m, 1H, *H*C-OP), 3.86- 3.91 (m, 1H, *H*C-OP), 3.99- 4.03 (m, 2H, *H2*C-OP), 5.24 (dd, 1H, *J* = 9.5 & 23.8 Hz, *H*C-P), 6.88 (d, 2H, *J* = 7.65 Hz, H-Ar), 7.33 (d, 2H, *J* = 7.65, H-Ar), 7.39-7.41(m, 3H, *J* = 7.65, 2H-Ar + N*H*), 7.51 (d, 2H, J = 8.60, H-Ar), 10.53 (s, 1H, N*H*-CP); ^{13}C NMR (125.7 MHz, DMSO): δ = 161.7, 156.5, 151.9, 151.8, 135.7, 132.8, 130.6, 130.5, 128.7, 126.8, 113.2, 104.9 (C-Ar), 63.28, 63.23, 63.06, 63.01 (2O*C*H_2), 53.1 (d, $^{1}J_{PC}$ = 152.2 Hz, *C*-P), 16.8, 16.7, 16.6, 16.5 (2OC-*C*H_3), 10.7, 6.1 (2*C*H_3); IR (KBr): 3444 (NH), 1349 (SO_2, asy), 1234 (P=O), 1164 (SO_2, sym), 1022 (P-O-C) cm^{-1}. Anal. calcd. for $C_{22}H_{27}ClN_3O_6PS$ (527.96): C, 50.05; H, 5.15; N, 7.96. Found: C, 49.87; H, 5.36; N, 8.12.

Diethyl (4-bromophenyl)(4-(N-(3,4-dimethylisoxazol-5-yl) sulfamoyl)phenylamino) methylphosphonate (**3h**) was obtained as grey crystals (0.99 g, 93%); mp 203-205°C (EtOH); ^{1}H NMR (500 MHz, DMSO): δ =1.04 (t, 3H, *H3*CCOP), 1.13 (t, 3H, *H3*CCOP), 1.47 (s, 3H, *H3*C), 2.00 (s, 3H, *H3*C), 3.74- 3.79 (m, 1H, *H*C-OP) 3.87- 3.92 (m, 1H, *H*C-OP), 3.39-4.04 (m, 2H, *H2*C-OP), 5.24 (dd, 1H, *J* = 9.5 & 24.8 Hz, *H*C-P), 6.89 (d, 2H, *J* = 7.6 Hz, H-Ar), 7.34 (d, 2H, *J* = 7.6 Hz, H-Ar), 7.45 (d, 2H, *J* = 8.6 Hz, H-Ar), 7.52

(d, 2H, J = 6.7 Hz, H-Ar), 10.54 (s, 1H, N*H*-CP); ^{13}C NMR (125.7 MHz, DMSO): δ = 161.6, 156.6, 151.9, 151.8, 136.1, 131.5, 130.97, 130.93, 128.7, 126.9, 121.4, 113.2, 104.9 (*C*-Ar), 63.29, 63.24, 63.06, 63.01 (2O*C*H$_2$), 53.8 (d, $^1J_{PC}$ = 152.2 Hz, *C*-P), 16.8, 16.7, 16.6, 16.5 (2OC-*C*H$_3$), 10.7, 6.2 (2*C*H$_3$); IR (KBr): 3297 (NH), 1349 (SO$_2$, asy), 1234 (P=O), 1164 (SO$_2$, sym), 1022 (2P-O-C) cm^{-1}; Anal. calcd. for $C_{22}H_{27}BrN_3O_6PS$ (572.41): C, 46.16; H, 4.75; N, 7.34. Found: C, 46.34; H, 4.54; N, 7.17.

Diethyl (4-cyanophenyl)(4-(N-(3,4-dimethylisoxazol-5-yl)-sulfamoyl)phenylamino) methylphosphonate (3i) was obtained as a white solid (0.84 g, 87%); mp 209-211°C (EtOH); ^{1}H NMR (500 MHz, DMSO): δ =1.04 (t, 3 H, *H*$_3$CCOP), 1.13 (t, 3 H, *H*$_3$CCOP), 1.47 (s, 3H, *H*$_3$C), 2.00 (s, 3H, *H*$_3$C), 3.76- 3.81 (m, 1H, *H*C-OP) 3.88- 3.93 (m, 1H, *H*C-OP), 4.00-4.04 (m, 2H, *H*$_2$C-OP), 5.38 (dd, 1H, J = 9.6 & 24.8 Hz, *H*C-P), 6.89 (d, 2H, J = 8.6 Hz, H-Ar), 7.33 (d, 2H, J = 7.6, H-Ar), 7.49 (t, 1H, N*H*), 7.68 (d, 2H, J = 7.6 Hz, H-Ar), 7.81(d, 2H, J = 7.6 Hz, H-Ar), 10.54 (s, 1H, N*H*-CP); ^{13}C NMR (125.7 MHz, DMSO): δ = 161.6, 156.5, 151.7, 151.6, 142.7, 132.5, 129.7, 129.6, 128.7, 127.2, 113.2, 111.0, 104.9 (*C*-Ar), 119.1 (*C*N), 63.49, 63.44, 63.19, 63.14 (2OC*H*$_2$), 53.8 (d, $^1J_{PC}$ = 150.2 Hz, *C*-P), 16.77, 16.74, 16.57, 16.55 (OC*C*H$_3$), 10.7, 6.2 (2*C*H$_3$); IR (KBr): 3421 & 3293 (NH), 2229 (CN), 1349 (SO$_2$, asy), 1234 (P=O), 1172 (SO$_2$, sym), 1045 (2P-O-C) cm^{-1}; Anal. calcd. for $C_{23}H_{27}N_4O_6PS$ (518.52): C, 53.28; H, 5.25; N, 10.81. Found: C 53.43; H, 5.06; N, 10.02.

Diethyl (4-(N-(3,4-dimethylisoxazol-5-yl)sulfamoyl)-phenylamino)(4-nitrophenyl) methylphosphonate (3j) was obtained as a yellow solid (0.88, 88%); mp 198-200°C (EtOH); ^{1}H NMR (500 MHz, DMSO): δ =1.06 (t, 3H, *H*$_3$CCOP), 1.15 (t, 3H, *H*$_3$CCOP), 1.49 (s, 3H, *H*$_3$C), 1.99 (s, 3H, *H*$_3$C), 3.79- 3.83 (m, 1H, *H*C-OP) 3.90- 3.96 (m, 1H, *H*C-OP), 4.01-4.06 (m, 2H, *H*$_2$C-OP), 5.49 (dd, 1H, J = 9.5 & 24.8 Hz, *H*C-P), 6.90 (d, 2H, J = 7.65 Hz, H-Ar), 7.34 (d, 2H, J = 7.65, H-Ar), 7.54 (t, 1H, N*H*), 7.76 (d, 2H, J = 8.6, H-Ar), 8.21 (d, 2H, J = 7.65, H-Ar), 10.54 (s, 1H, N*H*-CP); ^{13}C NMR (125.7 MHz, DMSO): δ = 161.6, 156.5, 151.7, 151.5, 147.4, 144. 8, 129.9, 128.7, 127.3, 123.7, 113.2, 104.9 (C-Ar), 63.57, 63.51, 63. 2, 63.1 (2O*C*H$_2$), 53.6 (d, $^1J_{PC}$ = 150.2 Hz, *C*-P), 16.79, 16.75, 16.6, 16.5 (OC*C*H$_3$), 10.7, 6.2 (2*C*H$_3$); Anal. calcd. for $C_{22}H_{27}N_4O_8PS$ (538.51): C, 49.07; H, 5.05; N, 10.40. Found: C, 48.88; H, 4.82; N, 10.58.

Diethyl (4-(N-(3,4-dimethylisoxazol-5-yl)sulfamoyl)pheny-lamino)(4-hydroxy-3-methoxyphenyl)methylphosphonate (3K) was obtained as a white solid (0.91 g, 90.5%); mp 212-214°C (EtOH); ^{1}H NMR (500 MHz, DMSO): δ =1.03 (t, 3H, *H*$_3$CCOP), 1.13 (t, 3H, *H*$_3$CCOP), 1.50 (s, 3H, *H*$_3$C), 2.01 (s, 3H, *H*$_3$C), 3.69-372 (m, 4H, *H*$_3$CO+ *H*C-OP) 3.84- 3.88 (m, 1H, *H*C-OP), 3.97-4.00(m, 2H, *H*$_2$C-OP), 5.00 (d, 1H, J = 5.5 & 16.2 Hz, *H*C-P), 6.68(s, 1H, *H*-Ar), 6.88 (s, 3H, *H*-Ar), 7.09 (s, 1H, H-Ar), 7.28 (s, 1H, N*H*), 7.33 (s, 2H, *H*-Ar), 8.95(s, br, 1H, O*H*), 10.50 (s, 1H, N*H*-CP); ^{13}C NMR (125.7 MHz, DMSO): δ = 161.7, 156.6, 152.19, 152.09, 147.8, 146.6, 128.6, 126.9, 126.4, 121.4, 115.5, 113.1, 113.0, 104.8 (C-Ar), 62.9, 62.8 (2O*C*H$_2$), 56.2 (O*C*H$_3$), 53.4 (d, $^1J_{PC}$ = 152.6 Hz, *C*-P), 16.86, 16.82, 16.67, 16.63 (2OC*C*H$_3$), 10.8, 6.2 (2*C*H$_3$); Anal. calcd. for $C_{23}H_{30}N_3O_8PS$ (539.54): C, 51.20; H, 5.60; N, 7.79. Found: C, 51.03; H, 5.41; N, 7.94.

Diethyl (4-chloro-3-nitrophenyl)(4-(N-(3,4-dimethylisoxazol-5-yl)sulfamoyl) phenylamino)methylphosphonate (3l) was ob-tained as a yellow solid (0.92 g, 86%); mp 195-197°C (EtOH); ^{1}H NMR (500 MHz, DMSO): δ =1.07 (t, 3H, *H*$_3$CCH$_2$OP), 1.14 (t, 3H, *H*$_3$CCH$_2$OP), 1.49 (s, 3H, *H*$_3$C), 2.00 (s, 3H, *H*$_3$C), 3.82- 3.87 (m, 1H, *H*C-OP) 3.93- 3.98 (m, 1H, *H*C-OP), 4.02-4.07 (m, 2H, *H*$_2$C-OP), 5.49 (dd, 1H, J = 9.5 & 15.2 Hz, *H*C-P), 6.91 (d, 2H, J = 8.6, H-Ar), 7.36 (d, 2H, J = 8.6, H-Ar), 7.49 (s (br), 1H, NH), 7.78-7.89 (m, 2H, H-Ar), 8.20 (s, 1H, H-Ar), 10.55 (s, 1H, N*H*-CP); ^{13}C NMR (125.7 MHz, DMSO): δ = 161.6, 156.5, 151.5, 151.4, 147.7, 138.4, 134.0, 132.1,129.2, 129.0, 128.8, 113.3, 113.2, 104.9 (C-Ar), 63.6, 63.5, 63.28, 63.22(2O*C*H$_2$), 52.7 (d, $^1J_{PC}$ = 150.2 Hz, *C*-P), 16.76, 16.73, 16.58, 16.51(2OC*C*H$_3$), 10.7, 6.3 (2*C*H$_3$); Anal. calcd. for $C_{22}H_{26}ClN_4O_8PS$ (572.96): C, 46.12; H, 4.57; N, 9.78; Found: C, 45.93; H, 4.73; N, 9.58.

Diethyl (4-(N-(3,4-dimethylisoxazol-5-yl)sulfamoyl)phenyl-amino)(2,4-dinitrophenyl) methylphosphonate (3m) was ob-tained as a white solid (0.93 g, 86%); mp 200-202°C (EtOH); ^{1}H NMR (500 MHz, DMSO): δ =1.11 (t, 3H, *H*$_3$CCH$_2$OP), 1.28 (t, 3H, *H*$_3$CCH$_2$OP), 1.79 (s, 3H, *H*$_3$C), 2.12 (s, 3H, *H*$_3$C), 3.87- 3.92 (m, 1H, *H*C-OP) 3.95- 3.99 (m, 1H, *H*C-OP), 4.15-4.21 (m, 2H, *H*$_2$C-OP), 5.56 (dd, 1H, J = 9.7 & 19.2 Hz, *H*C-P), 6.70 (d, 2H, J = 8.6, H-Ar), 7.53 (d, 2H, J = 8.5, H-Ar), 7.79-7.91 (m, 3H, 2H-Ar + NH), 8.31 (s, 1H, H-Ar), 10.52 (s, 1H, N*H*-CP); ^{13}C NMR (125.7 MHz, DMSO): δ = 161.9, 155.4, 155.2, 149.6, 149.2, 147.6, 138.0, 136.4, 134.2, 129.5, 12.89, 127.7, 113.2,112.9, 106.5 (C-Ar), 63.6, 63.5, 63.28, 63.22(2O*C*H$_2$), 52.7 (d, $^1J_{PC}$ = 150.2 Hz, *C*-P), 16.76, 16.73, 16.58, 16.51(OC*C*H$_3$), 10.7, 6.5 (2*C*H$_3$); Anal. calcd. for $C_{22}H_{26}N_5O_{10}PS$ (583.51): C, 45.28; H, 4.49; N, 12.00. Found: C, 45.09, H; 6.41; N, 12.18.

2.1.2. Antimicrobial activity

The antimicrobial activities of compounds **3a-3m** were exam-ined against some targeted pathogenic microorganisms obtained from the American type culture collection (ATCC; Rockville, MD, USA). The organisms used were *S. aurous* ATCC- 47077 (St.), *L. monocytogenes* ATCC- 35152 (List.), *E. coli* ATCC-25922 (E.C.), *S. typhi* ATCC-15566 (Salm.) and *C. albicans* ATCC-10231 (C. Alb.) [53,54] The stock cultures of pathogens used in this study were maintained on nutrient agar slants at 4°. The Agar well diffusion method was employed to study the antimicrobial activities **3a-3m** according to a reported method [55,56]. Reference antibacte-rial drugs ampicillin and vancomycin were evaluated for their an-tibacterial and antifungal activities and compared with the starting compound, sulfisoxazole, and compounds **3a-3m**. Seventy micro-liters of bacterial and yeast cells (10^6 CFU/mL) of each pathogen were spread on the nutrient agar plates. The wells (6 mm diame-ter) were dug on the inoculated agar plates and 100 µL of sulfisox-azole and compounds **3a-3m** suspended in DMSO (100 mg/ml), were added to the wells. The reference antibiotics disks (10 and 30 µg/disk of ampicillin and vancomycin, respectively) were pot-ted onto the surface of the agar inoculated plates. The plates were allowed to stand at 4°C for 2 h before incubation to allow for dif-fusion. The plates were incubated at 37°C for 24 h, (except yeast strain which was incubated at 28°C for 24 h) then followed by the measurement of the diameter of the inhibition zone (mm), and three replicates were averaged [57].

Determination of Minimum Inhibition Concentration (MIC)

The MIC calculation of the tested compounds was performed according the reported method [58,59]. In brief, serial dilutions of the tested materials were prepared by dissolution in DMSO. A 150 μL volume of double strength Mueller Hinton broth medium was loaded in each well of the 96 well microtiter plate followed by 150 μL of the 2 fold appropriate concentration and mix well to ob-tain the final concentration. Overnight broth cultures of the tested bacterial and yeast strains prepared as an inoculum of 5 % (V/V) (OD = 0.5 McFarland standard) was inoculated into the respective wells. For the positive growth control, the same inoculum size of each test strain was inoculated in wells that didn't containing any of the tested substance. DMSO solution was tested as negative con-trol. The plates were statically incubated at 37°C for 24 h. A 30 μL of resazurin solution (0.18 %) was added to each well to act as an electron acceptor and reduce to a pink, red or purple resorufin col-ored product by active microorganisms (i.e. inhibition of bacterial growth was visible as a dark blue well and the presence of growth was detected by the presence of pink, red or purple color). The MIC

.

Table 1
Synthesis of diethyl (4-(N-(3,4-dimethylisoxazol-5-yl)sulfamoyl)phenyl-amino) (phenyl) methyl-phosphonate (**3a**) under different reaction conditions.

Entry	Catalyst	Reaction conditions	Isolated yield of **3a**
1	$Fe(OTf)_2$	r.t., overnight	——
2	$Fe(OTf)_2$	Reflux, 24h	40 %
3	$Fe(OTf)_2$	MWI, 70 °C, 70 min	70 %
4	AgOTf	MWI, 70 °C, 60 min	76%
5	$Cu(OTf)_2$	MWI, 70 °C, 60 min	80%
6	$Bi(OTf)_3$	MWI, 70 °C, 45 min	88%

was defined as the concentration at which the bacteria and yeast did not show visible growth with respect to the positive control.

2.1.3. QSAR modelling

Described in supplementary section S1.

2.1.4. Crystal structure determination

Described in supplementary section S2. The crystal structure has been deposited in the CSD with reference numbers CCDC 2087290.

3. Results and discussion

3.1. Chemistry

In order to optimize the reaction conditions, the one-pot three component reaction between sulfisoxazole (**1**), benzaldehyde (**2a**) and diethylphosphite was considered as a model example. First, the reaction was investigated under conventional heat and under microwave irradiation (MWI) conditions in the presence of iron (II) trifluoromethanesulfonate $Fe(OTf)_2$ as a catalyst (Table 1, entries 1-3). The isolated yields of diethyl (4-(N-(3,4-dimethylisoxazol-5-yl)sulfamoyl)phenylamino) (phenyl)methylphosphonate (**3a**) show that the microwave irradiation reaction (entry 3) outperforms con-ventional heating Scheme 1.

The next step aimed to determine the best triflate catalyst for the reaction (Table 1, entries 3-6). The results show that the use of $Bi(OTf)_3$ as the catalyst under microwave irradiation was the most effective (entry 6).

The deduced optimum conditions were then applied to the condensation reaction of sulfisoxazole (**1**), diethyl phosphite, and several electron-donating /withdrawing substituted benzaldehy-des **2b-2m**. The investigation was under microwave irradiation in ethanol at 70°C, in the presence of $Bi(OTf)_3$ as the catalyst (Scheme 2).

The chemical identities of the synthesized α-aminophosphonates **3** were confirmed by spectroscopy. Com-pounds **3a-3m** displayed a doublet signal in ^{13}C NMR spectra, in each case, due to the formed chiral carbon atom (N-CH-P) at $\delta_C \approx$ 52-53 ppm with $^1J_{P-C} \approx$ 149-152 Hz. In compound **3g**, for example, ^1H NMR showed the two chemically non-equivalent ethoxy-methyl groups (H_3CCH_2OP) as triplets at 1.04 and 1.13 ppm.

The two ethoxy-methylene phosphonate groups behave differently. One of groups appears as a multiplet at δ = 3.99-4.03 (2H, H_2C-OP), while the two protons of the other ethoxy-methylene group resonate as two split quadruplets, as a result of their different environments, at 3.73-3.78 (m, 1H, *H*C-OP) and 3.86- 3.91 (m, 1H, *H*C-OP) ppm. The P-C-H proton appears as a doublet of doublets at δ = 5.24 ppm (J = 9.5 & 23.8 Hz). The correlation between the neighbouring ethoxy phosphonate groups was shown by 2D NMR (^1H-^1H Cosy and HSQC, supplementary Figs. S16 & S17). The structure of **3g** was also confirmed by single crystal diffraction (Fig. 3).

It is notable that the N-H proton of sulfonamide group expected to be observed downfield (compared with the other NH group) is absent from the ^1H-NMR data of compounds **3h**. It is likely that the NH signal is masked under water of DMSO, while the aminophosphonate NH group appears upfield at ≈ 10 ppm. A sim-ilar observation has been documented for sulfisoxazole derivatives [60].

3.2. Single crystal X-ray diffraction study

The crystal structure has been determined and the data col-lection and refinement information is presented in supplementary section S2. The asymmetric unit of the crystal structure is shown in Fig. 3. The structure contains a 1:1 mixture of **3g** and DMF sol-vent. An intramolecular N-H…O contact occurs in the molecule of **3g**, with geometry: N3-H3…O4 = 130.0°, N3…O4 = 2.930(4) Å. In the molecule, the planes of the oxazolyl (C2-C5, O1, N1) ring and one phenyl (C13-C18) group are parallel and separated by a dis-tance of 7.1Å. The two groups are essentially perpendicular to the plane of the second phenyl ring (C6 – C11). Intermolecular hydro-gen bonding between the molecule of **3g** and DMF molecule is ob-served, with geometry: N2-H2…O7 = 2.728(3)°, N2…O7 = 141.8 Å.

3.3. Biological evaluation

Antimicrobial evaluation

The antimicrobial properties of the synthesized compounds and sulfisoxazole were qualitatively and quantitatively assessed by *in-vitro* standard techniques utilizing five pathogenic microorgan-isms obtained from the American type culture collection (ATCC; Rockville, MD, USA). The organisms used are two Gram-positive bacteria (*S. aurous* ATCC-47077 (St.) and *L. monocytogenes* ATCC-35152 (List.)), two Gram-negative bacteria (*E. coli* ATCC25922 (E.C.) and *S. typhi* ATCC-15566 (Salm.)) and yeast *C. albicans* ATCC-10231 (C. Alb.) (Tables 2 and 3).

Gram-negative bacteria

Generally, all the synthesized agents revealed excellent activi-ties (compound **3k** is an exception) when tested against *S. typhi* pathogen. Compound **3m** (R & R^2 = NO_2, R^1 = H) is very effec-tive and shows about 2.1 times the potency of the sulfisoxazole (MIC = 94.2 and 205.7 µM for **3m** and sulfisoxazole, respectively)). Compounds **3a, 3h, 3j**, and **3l** exhibited higher MIC values (121.6, 131.0, 111.4 and 151.8 µM respectively).

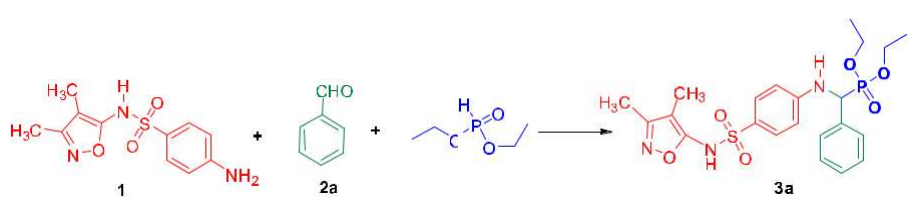

Scheme 1. Synthesis of α-aminophosphonate **3a**.

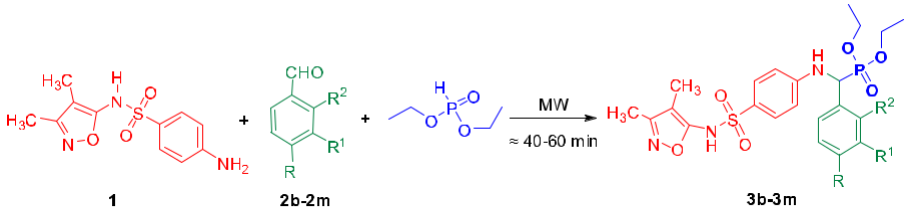

2, 3b; R = Me, $R^1 = R^2 = H$ **2, 3h;** R = Br, $R^1 = R^2 = H$
2, 3c; R = OMe, $R^1 = R^2 = H$ **2, 3i;** R = CN, $R^1 = R^2 = H$
2, 3d; R = OH, $R^1 = R^2 = H$ **2, 3j;** R = NO_2, $R^1 = R^2 = H$
2, 3e; R = NMe_2, $R^1 = R^2 = H$ **2, 3k;** R = OH, R^1 = OMe, $R^2 = H$
2, 3f; R = F, $R^1 = R^2 = H$ **2, 3l;** R = Cl, $R^1 = NO_2$, $R^2 = H$
2, 3g; R = Cl, $R^1 = R^2 = H$ **2, 3m;** R, $R^2 = NO_2$, $R^1 = H$,

Scheme 2. Synthesis of the target α-aminophosphonates **3b-3m**.

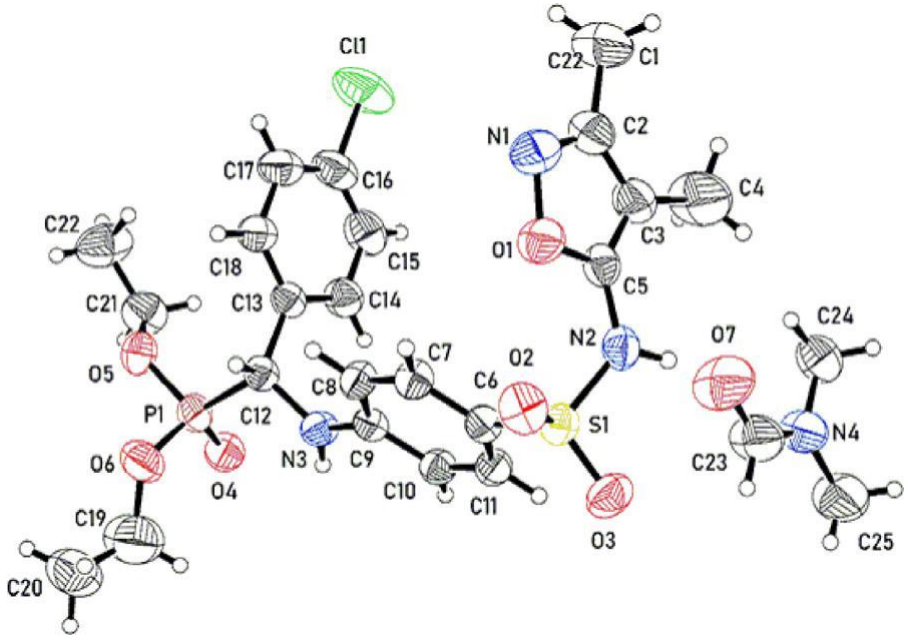

Fig. 3. Ortep representation of compound **3g**.

Table 2

Antimicrobial activity expressed as inhibition diameter zones in millimeters (mm) (include well diameter) for the synthesized compounds at 100 mg/ml against the pathological strains based on well diffusion method). Ampicillin and vancomycin are used as reference drugs.

Compound No	*E. coli*	*S. Typhi*	*S. aureus*	*L. monocytogenes*	*C. albicans*
3a	13	20	6	10	6
3b	6	11	6	6	9
3c	6	11	10	8	12
3d	6	8	6	9	6
3e	6	11	11	9	12
3f	6	12	6	9	6
3g	6	8	6	10	6
3h	15	15	10	12	10
3i	6	8	6	6	10
3j	19	20	13	18	13
3k	6	6	6	6	6
3l	20	9	6	14	13
3m	28	23	16	20	18
Sulfisoxazole	25	23	14	25	15
Ampicillin	16	19	15	20	9
Vancomycin	15	17	14	15	15

Some structure activity relationships (SARs) can be deduced from the results. The substituted phenyl analogs possess in-hibitory activity lower than the unsubstituted phenyl analog **3a** (MIC = 121.6 μM), except in case of para-nitro substituted phenyl analogs **3m** and **3j** (MIC = 94.2 and 111.4 μM, respec-tively). It is probable that the potent inhibitory activity of **3m** (R & $R^2 = NO_2$, R^1 = H) is due to the presence of two nitro groups.

In case of *E. coli*, only **3a, 3h, 3j, 3l**, and **3m** displayed signif-icant inhibitory activities. The most active analogs are those that contain nitro group(s) **3m** > **3l** > **3j** with MIC values of 85.7, 104.7 and 111.4 μM, respectively whereas the MIC value for sulfisoxazole

Table 3
Minimum inhibitory concentrations (MIC) represented in mg/ml, (μM) of the synthesized compounds against the pathogenic strains based on two-fold serial dilution technique.

Compound No.	Gram (-ve) pathogenic bacteria MIC mg/ml (μM)		Gram (+ ve) pathogenic bacteria MIC mg/ml (μM)		MIC mg/ml (μM)
	E. coli	*S. typhi*	*S. aureus*	*L. monocytogenes*	*C. albicans*
3a	80 (162.1)	60 (121.6)	> 100 (>202.6)	85 (172.2)	> 100 (>202.6)
3b	> 100 (>197.0)	85 (167.5)	> 100 (>197.0)	> 100 (>197.0)	87 (171.4)
3c	> 100 (>191.0)	85 (162.3)	85 (162.3)	90 (171.9)	80 (152.8)
3d	> 100 (>196.3)	90 (176.6)	> 100 (>196.3)	87 (170.7)	> 100 (>196.3)
3e	> 100 (>186.4)	85 (158.4)	85 (158.4)	87 (162.1)	80 (149.0)
3f	> 100 (>195.5)	80 (156.4)	> 100 (>195.5)	87 (170.0)	> 100 (>195.5)
3g	> 100 (>189.4)	90 (170.5)	> 100 (>189.4)	85 (161.0)	> 100 (>189.4)
3h	75 (131.0)	75 (131.0)	85 (148.5)	80 (139.7)	85 (148.5)
3i	> 100 (>192.8)	90 (173.6)	> 100 (>192.8)	> 100 (>192.8)	85 (163.9)
3j	60 (111.4)	60 (111.4)	80 (148.5)	65 (120.7)	80 (148.5)
3k	>100 (>185.3)	>100 (>185.3)	>100 (>185.3)	>100 (>185.3)	>100 (>185.3)
3l	60 (104.7)	87 (151.8)	> 100 (> 174.5)	75 (130.9)	80 (139.6)
3m	50 (85.7)	55 (94.2)	70 (119.9)	60 (102.8)	65 (111.4)
Sulfisoxazole	50 (187.0)	55 (205.7)	75 (280.5)	50 (187.0)	75 (280.6)

is 187.0 μM. It is also noted that the unsubstituted phenyl ana-log **3a** is the least potent among the reported active compounds (MIC = 162.1, 131.0, 111.4, 104.7 and 85.7 μM for **3a, 3h, 3j, 3l**, and **3m,** respectively).

In general, we can adduce that the presence of nitro group(s) in the phenyl moiety (especially in the para-position) plays a signif-icant role in enhancement of the inhibitory properties of the syn-thesized analogs against Gram-negative strains.

Gram-positive bacteria

All the tested compounds demonstrate high inhibitory activi-ties (compounds **3a** and **3i** are exceptions) when tested against *L. monocytogenes*. Compounds **3m, 3j, 3l**, which are nitro substituted derivatives, are the most potent agents (with MIC values of 102.8, 120.7, 130.9 and 187.0 μM for **3m, 3j, 3l** and sulfisoxazole, respec-tively).

The deduced SAR shows the effective role of the presence of the nitro group as substituent, especially in para-position (**3m** and **3j**). The order of the activities is **3m** > **3j** > **3l**. The efficacy of halo-substituted phenyl derivatives **3f, 3g, 3h** is in the order, bro-mophenyl > chlorophenyl > fluorophenyl, which is opposite to the -I effect of the halogen atom.

In the case of *S. aureus*, only **3c, 3e, 3h, 3j**, and **3m** are consid-erable, with MIC values of 162.3, 158.4, 148.5, 148.5 and 119.9 μM, respectively while the MIC value of sulfisoxazole is 280.5 μM. It is also notable that **3m** is the most effective inhibitor (R & R^2 = NO_2, R^1 = H).

albicans

Most of the tested compounds show high potency as *C. albicans* inhibitors. The highest values are for **3m, 3l, 3j** (nitro substituted derivatives) and **3h** with MIC values of 111.4, 139.6, 148.5, 148.5 and 280.6 μM for **3m, 3l, 3j, 3h** and sulfisoxazole, respectively.

3.4. QSAR studies

QSAR (quantitative structure-activity relationship) is a molec-ular modelling technique adoptable for medical chemical studies to rationalize the parameters associated with biological proper-ties [61,62]. The biological properties are expressed as descriptor (physico-chemical) values and thus the bio-properties can be quan-titatively determined mathematically [63].

S. typhi

The synthesized compounds **3a-3j, 3l, 3m** and sulfisoxa-zole were considered using the CODESSA-Pro software [64] for

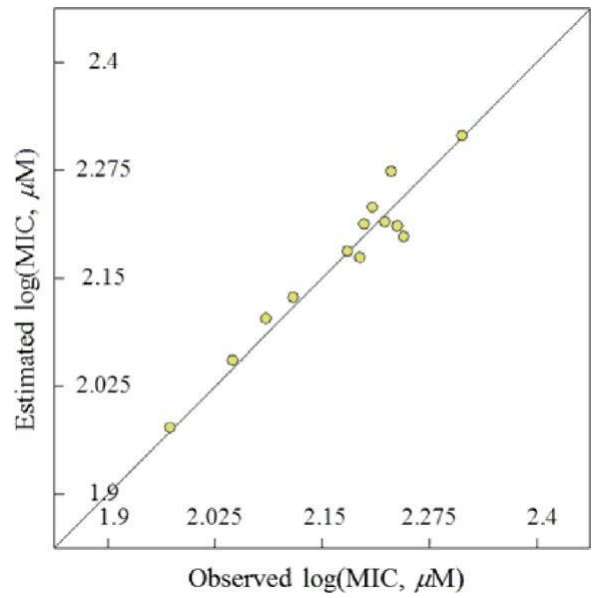

Fig. 4. QSAR plot representing the observed versus predicted log(MIC, μM) for the agents tested against *S. typhi*.

QSAR modelling. The robust QSAR model (R^2=0.937 R^2_{cv}00=0.902, R^2_{cv}MO = 0.913) covers a wide range of antibacterial properties ($MIC_{observed}$ = 94.2–205.7, $MIC_{estimated}$ = 94.7–205.8 μM) (Supple-mentary Tables S1-S3, Fig. 4).

Minimum exchange energy for bond H-C is a semi-empirical descriptor with a coefficient value of 1.17262. A high mathemati-cal descriptor value for an agent represents low potent antibacte-rial properties as shown by **3m** and sulfisoxazole (descriptor val-

ues = 4.9926 and 5.2426; $MIC_{estimated}$ = 93.4 and 207.7 μM, for compound **3m** and sulfisoxazole, respectively). The electronic ex-

change energy between two different atoms can be calculated by equ. (1) [65].

$$E_{exc}(AB) = \sum_{\mu,\nu \in A} \sum_{\lambda,\sigma \in B} P_{\mu\lambda} P_{\nu\sigma} \langle \mu\lambda | \nu\sigma \rangle \quad (1)$$

where, *A* and *B* are two different atoms. $P_{\mu\nu}$, $P_{\lambda\sigma}$; $\langle \mu\nu | \lambda\sigma \rangle$ are the density matrix elements and electron repulsion integrals, re-spectively on the atomic basis $\{\mu\nu\lambda\sigma\}$.

Minimum coulombic interaction for bond H-N is also a semi-empirical descriptor with the highest coefficient value (1.48809). Again, a higher mathematical descriptor value leads to weaker an-

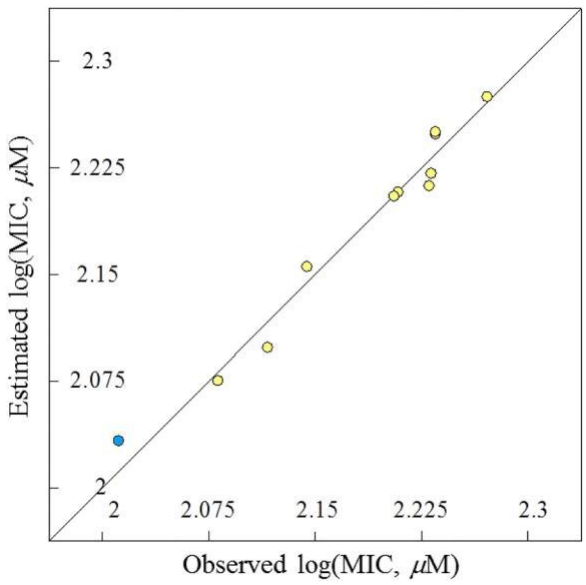

Fig. 5. QSAR plot representing the observed versus predicted log(MIC, μM) for the agents tested against *L. monocytogenes* (compound **3m** is an outlier).

tibacterial activity as shown in compounds **3e** and **3m** (descriptor values = 4.2414 and 4.1887; $MIC_{estimated}$ = 176.4 and 93.4 μM for compounds **3e** and **3m**, respectively). The coulombic interactions are mainly electrostatic interactions between electric charges [66]. The total interaction energy between two different atoms can be calculated by equ. (2) [65].

$$E_{tot}(AB) = E_C(AB) + E_{exc}(AB) \quad (2)$$

where, A and B are two different atoms. $E_C(AB)$ and $E_{exc}(AB)$ are the electrostatic interaction and exchange energies between the two different atoms.

Total dipole of the molecule is also a semi-empirical descrip-tor with a negative coefficient value (-0.0343854). This explains the high efficacy of the agent with high mathematical descriptor value as shown by compounds **3c** and **3m** (descriptor value = 2.306 and 7.47; corresponding for estimated MIC value = 170.3 and 94.7 μM for compounds **3c** and **3m**, respectively). The dipole moment of a molecule can be calculated by equ. (3) [65].

$$\mu = -\sum_{i=1}^{occ} \int_{(V)} \varphi_i \hat{r} \varphi_i dV + \sum_{a=1}^{M} Z_a R_a \quad (3)$$

where, φ_i are the molecular orbitals, $\hat{r}$ is the electron position op-erator, Z_a is the ath atomic charge and R_a is the position vector of ath atomic nucleus.

L. monocytogenes

The two-descriptor QSAR model describes the antibacterial properties of the tested agents **3a, 3c–3h, 3j, 3l, 3m** and sulfisoxazole with good coefficient parameters (R^2 = 0.971, R^2cvOO = 0.939, R^2cvMO = 0.953)) (Supplementary Tables S4-S6, Fig. 5). The model covers a wide range of antibacterial properties ($MIC_{observed}$ = 102.8–187.0, $MIC_{estimated}$ = 107.8–188.0 μM) includ-ing the potent analogues relative to the standard reference used (sulfisoxazole).

The area-weighted surface charge of hydrogen bonding accep-tor atoms (HASA-2) over total molecular surface area (TMSA) is a charge-related descriptor with a negative sign coefficient value (-6.94591). This explains the high efficacy of the agent with high mathematical descriptor values as shown by compounds **3a** and **3m** (descriptor value = 0.03303 and 0.063 corresponding to esti-mated MIC = 177.3 and 107.8 μM for compounds **3a** and **3m**, re-spectively). The HASA-2 can be calculated by equ. (3) [65].

$$HASA-2 = \sum_A q_A \sqrt{\frac{S_A}{S_{tot}}} \quad (3)$$

where, S_A is the solvent accessible surface area of the hydrogen-bonding acceptor atoms and q_A is the partial charge on the hydrogen-bonding acceptor atoms. The S_{tot} is the total solvent ac-cessible surface area of the molecule.

The WPSA3 (surface weighted partial charged surface area) is also a charge-related descriptor with a negative sign coefficient value (-0.00466243). This rationalizes the high efficacy of com-pound **3m** over **3b** (descriptor values = 56.19756 and 70.25735; MIC value = 178.0 and 107.8 μM for compounds **3b** and **3m**, re-spectively). The WPSA3 can be calculated by equ. (4) [65].

$$WPSA3 = \frac{PPSA3}{TMSA} \quad (4)$$

where PPSA3 is the weighted total partial positively charged sur-face area of the molecule and TMSA is the total molecular surface area.

The comparative estimated antimicrobial properties relative to the observed values support the goodness of the QSAR models. The high correlation coefficient values of both leave-one-out (R^2cvOO) and leave-many-out (R^2cvMO) relative to the original QSAR models are also good evidence for the computational models (Supplemen-tary Tables S1–S6, Figs. 4, 5).

4. Conclusion

In summary, a new series of α-aminophosphonate derivatives **3a-3m** based on sulfisoxazole were synthesized through the one-pot Kabachnik-Fields reaction of sulfisoxazole, diethyl phosphite (DEP) and substituted aldehydes. The reaction conditions were op-timized, it was found to be the use of bismuth (III) triflate as a cat-alyst under microwave irradiation. The conditions gave the target compounds in excellent yields. The antimicrobial properties of the new synthesized agents were tested against five pathogenic mi-croorganisms. Compound **3m** exhibited the most promising prop-erties with potent antibacterial activity against all the tested mi-croorganisms. The observed biological properties are supported by QSAR models Fig. 2.

CRediT authorship contribution statement

Dr. Eman sabry: Conceptualization; Methodology, Investigation, Visualization, Writing - Reviewing and Editing; **Dr. Hanan Mo-hamed:** Investigation, Writing - Original draft preparation; **Dr. Ewies F. Ewies:** Resources, Investigation, Writing - Original draft preparation; **Prof. Benson Kariuki:** Methodology, Investigation, Performed the X-ray studies, Writing - Reviewing and Editing, Su-pervision of language; **Dr. Osama M. Darwesh:** Performed the an-timicrobial studies, Writing - Original draft preparation; **Dr. Mo-hamed Bekheit:** Conceptualization, Supervision, Methodology, In-vestigation, Visualization, Software, Writing - Reviewing and Edit-ing.

Declaration of Competing Interest

There is no conflict of interest

.

Data Availability

The data is available in supporting informations

Acknowledgement

We are thankful to National Research Centre for support.

Supplementary materials

Supplementary material associated with this article can be found, in the online version, at doi:

References

[1] H. Qadri, A.H. Shah, M. Mir, Novel strategies to combat the emerging drug resistance in human pathogenic microbes, Curr. Drug. Targets 22 (2021) 1424– 1436, doi:10.2174/1389450121666201228123212.

[2] W. Huai, Q-B Ma, J-J Zheng, Y. Zhao, Q-R Zhai, Distribution and drug resistance of pathogenic bacteria in emergency patients, World J. Clin. Cases 7 (2019) 3175–3184, doi:10.12998/wjcc.v7.i20.3175.

[3] Interagency Coordination Group on Antimicrobial Resistance, in: No time to wait: securing the future from drug-resistant infections. Report to the secre-tary-general of the United Nations, IACG, 2019, p. 28.

[4] Y. Wang, T.B. Oppong, X.L.G. Duan, H. Yang, Methicillin-resistant *Staphylococ-cus aureus* and vancomycin-resistant *Enterococci* co-colonization in patients: A meta-analysis, Am. J. of Inf. Control 48 (2020) 925–932, doi:10.1016/j.ajic.2019. 11.010.

[5] L.M. Abbo, E.J. Ariza-heredia, Antimicrobial stewardship in immunocompro-mised hosts, Infect. Dis. Clin. North. Am. 28 (2014) 263–279, doi:10.1016/j.idc. 2014.01.008.

[6] N. Jackson, L. Czaplewski, L.J.V. Piddock, Discovery and development of new antibacterial drugs: learning from experience? Antimicrob. Chemother. 73 (2018) 1452–1459, doi:10.1093/jac/dky019.

[7] M.I. Konaklieva, Addressing antimicrobial resistance through new medicinal and synthetic chemistry strategies, SlAS Discovery 24 (2019) 419–439, doi:10.1177/2472555218812657.

[8] G. Bérubé, An overview of molecular hybrids in drug discovery, Expert Opin. Drug Discov. 11 (2016) 281–305, doi:10.1517/17460441.2016.1135125.

[9] R.S. Vardanyan, V.J. Hruby, Synthesis of essential drugs, in: R.S. Vardanyan, V.J. Hruby (Eds.), 33-Antimicrobial Drugs, 2006, pp. 499–523, doi:10.1016/ B978-044452166-8/50033-9.

[10] A. Bonardi, A. Nocentini, S. Bua, J. Combs, C. Lomelino, J. Andring, L. Lucarini, S. Sgambellone, E. Masini, R. McKenna, P. Gratteri, C.T. Supuran, Sulfonamide Inhibitors of Human Carbonic Anhydrases Designed through a Three-Tails Ap-proach: Improving Ligand/Isoform Matching and Selectivity of Action, J. Med. Chem. 63 (2020) 7422–7444, doi:10.1021/acs.jmedchem.0c00733.

[11] R.A. Azzam, H.A. Elboshi, G.H. Elgemeie, Novel Synthesis and Antiviral Eval-uation of New Benzothiazole-Bearing N-Sulfonamide 2-Pyridone Derivatives as USP7 Enzyme Inhibitors, ACS Omega 5 (2020) 30023–30036, doi:10.1021/ acsomega.0c04424.

[12] A.A-M Abdel-Aziz, A. Angeli, A.S. El-Azab, M.E.A. Hammouda, M.A. El-Sherbeny, C.T. Supuran, Synthesis and anti-inflammatory activity of sulfonamides and carboxylates incorporating trimellitimides: Dual cyclooxygenase/carbonic an-hydrase inhibitory actions, Bio. Chem. 84 (2019) 260–268, doi:10.1016/j.bioorg. 2018.11.033.

[13] M.V. Kachaeva, D.M. Hodyna, I.V. Semenyuta, S.G. Pilyo, V.M. Prokopenko, V.V. Kovalishyn, L.O. Metelytsia, V.S. Brovarets, Design, synthesis and evalua-tion of novel sulfonamides as potential anticancer agents, Computational Bi-ology and Chemistry 74 (2018) 294–303, doi:10.1016/j.compbiolchem.2018.04. 006.

[14] C. Camoutsis, A. Geronikaki, A. Ciric, M. Sokovic, P. Zoumpoulakis, M. Zervou, Chem. Pharm. Bull. 58 (2010) 160–167, doi:10.1016/j.ejmech.2021.113837.

[15] https://go.drugbank.com/drugs/DB00263

[16] P.A. Turhanen, K.D. Demadis, P. Kafarski, Editorial: Phosphonate Chemistry in Drug Design and Development, Front. Chem. 9 (2021) 1–2, doi:10.3389/fchem. 2021.695128.

[17] A. Amira, Z. Aouf, H. K'tir, Y. Chemam, R. Ghodbane, R. Zerrouki, N-E. Aou, Re-cent Advances in the Synthesis of α-Aminophosphonates: A Review, Chemistry Select 6 (2021) 6137–6149, doi:10.1002/slct.202101360.

[18] K.M. Heidel, C.S. Dowd, phosphonate prodrugs: an overview and recent ad-vances, Future Med. Chem. 11 (2019) 1625–1643, doi:10.4155/fmc-2018-0591.

[19] O.I. Kolodiazhnyi, Phosphorus Compounds of Natural Origin: Pre-biotic, Stereochemistry, Application, Symmetry 13 (2021) 889-941. https://doi.org/10.3390/sym13050889.

[20] L. Xu, H. Wang, Z. Chu, L. Cai, H. Shi, C. Zhu, D. Pan, J. Pan, X. Fei, Y. Lei, Temperature-responsive multilayer films of Micelle-Based composites for con-trolled release of a third-generation EGFR inhibitor, ACS Appl. Polym. Mater. 2 (2020) 741–750, doi:10.1021/acsapm.9b01051.

[21] A. Mucha, P. Kafarski, Ł. Berlicki, Remarkable potential of the aminophospho-nate/phosphinate structural motif in medicinal chemistry, J. Med. Chem. 54 (2011) 5955–5980, doi:10.1021/jm200587f.

[22] P. Kafarski, B. Lejczak, Aminophosphonic acids of potential medical impor-tance, Curr. Med. Chem. Anticancer Agents 1 (2001) 301–312, doi:10.2174/ 1568011013354543.

[23] E.W. Logusch, D.M. Walker, J.F. McDonald, J.E. Franz, J.J. Villafranca, C.L. Di-Ianni, J.A. Colanduoni, J.B. Schineller, Inhibition of Escherichia coli glutamine synthetase by alpha- and gamma-substituted phosphinothricins, Biochemistry 29 (1990) 366–372, doi:10.1021/bi00454a009.

[24] X-C Huang, M. Wang, Y-M Pan, X-Y Tian, H-S Wang, Y. Zhang, Synthesis and antitumor activities of novel α-aminophosphonates dehydroabietic acid derivatives Bioorganic Med, Chem. Lett. 23 (2013) 5283–5289, doi:10.1016/j. bmcl.2013.08.005.

[25] M. Gnant, P. Clézardin, Direct and indirect anticancer activity of bisphospho-nates: A brief review of published literature, Cancer Treat. Rev. 38 (2012) 407– 415, doi:10.1016/j.ctrv.2011.09.003.

[26] J. Ma, J. Li, P. Guo, X. Liao, H. Cheng, Synthesis and antitumor activity of novel indole derivatives containing α-aminophosphonate moieties, Arab. J. Chem. 14 (2021) 103256, doi:10.1016/j.arabjc.2021.103256.

[27] S.U. Deshmukh, K.R. Kharat, A.R. Yadav, S.U. Shisodia, M.G. Damale, J.N. Sangeshetti, R.P. Pawar, Synthesis of Novel α-Aminophosphonate Deriva-tives, Biological Evaluation as Potent Antiproliferative Agents and Molecular Docking, ChemistrySelect 3 (2018) 5552–5558, doi:10.1002/slct.201800798.

[28] P. Sreelakshmi, M.R. Nadiveedhi, S. Santhisudha, G. Mohan, N. Saichaithanya, M. Sadik, K. Peddanna, S.R. Cirandur, Nano Sb_2O_3 catalyzed green synthesis, cy-totoxic activity, and molecular docking study of novel α-aminophosphonates, Med. Chem. Res. 28 (2019) 528–544, doi:10.1007/s00044-019-02302-y.

[29] M. Sienczyk, J. Oleksyszyn, Irreversible inhibition of serine proteases-design and in vivo activity of diaryl α-aminophosphonate derivatives, Current Med. Chem. 16 (2009) 1673–1687, doi:10.2174/092986709788186246.

[30] B. Ewa, W. Maciej, S.C. Marcin, D. Grzegorz, Z. Michał, P. Jan, O. Jozef, The de-velopment of first Staphylococcus aureus SplB protease inhibitors: Phospho-nic analogues of glutamine, Bioorganic Med. Chem. Lett. 22 (2012) 5574–5578, doi:10.1016/j.bmcl.2012.07.011.

[31] B. Litim, Z. Cheraiet, S. Meliani, A. Djahoudi, A. Boukhsri, Synthesis and potent antimicrobial activity of novel coumarylthiazole α-aminophosphonate deriva-tives, Mol. Divers. 26 (2022) 1161–1174, doi:10.1007/s11030-021-10242-2.

[32] S. Poola, S. Nagaripati, S. Tellamekala, V. Chintha, P. Kotha, J.R. Yagani, N. Golla, S.R. Cirandur, Grenn synthesis, antibacterial, antiviral and molecular dock-ing studies of α-aminophosphonates, Synth. Commun. 50 (2020) 2655–2672, doi:10.1080/00397911.2020.175307.

[33] S. Shaikh, P. Dhavan, G. Pavale, M.M. Ramana, B.L. Jadhav, Design, synthesis and evaluation of pyrazole bearing α-aminophosphonate derivatives as potential acetylcholine esterase inhibitors against Alzheimer's disease, Bioorg Chem 96 (2020) 103589, doi:10.1016/j.bioorg.2020.103589.

[34] D.A. Elsherbiny, A.M. Abdelgawad, M.E. El-Naggar, R.A. El-Sherbiny, M.H. El-Rafie, I.E-T. El-Sayed, Synthesis, antimicrobial activity, and sustainable release of novel α-aminophosphonate derivatives loaded carrageenan cryoge, Int. J. Biol. Macromol. 163 (2020) 96–107, doi:10.1016/j.ijbiomac.2020.06.251.

[35] A. Salin, A. Il'in, G. Fanuza, A. Fatkhutdinov, D. Islamov, O. Kataeva, V. Galkin, The Pudovik Reaction Catalyzed by Tertiary Phosphines, Curr. Org. Synth. 13 (2015) 132–141, doi:10.2174/1570179412999150723154625.

[36] T. Shilpa, N.A. Harry, S.M. Ujwaldev, G. Anilkumar, An Overview of Microwave-Assisted Kabachnik-Fields ChemistrySelect 5 (2020) 4422-4436. doi:10.1002/slct.202000693

[37] M.S. Bekheit, A.A. Kamel, Multi-Component Reactions in the Preparation of α-and β-Substituted Phosphonates, Curr. Org. Chem. 21 (2017) 923–938, doi:10.2174/1385272821666170113114456.

[38] G.K.S. Prakash, T. Mathew, G.A. Olah, Gallium(III) triflate: an efficient and a sustainable Lewis acid catalyst for organic synthetic transformations, ACC. Chem. Res. 17 (2012) 565–577, doi:10.1021/ar2002039.

[39] V. Ladziata, Recent applications of rare-earth metal(III) triflates in cycload-dition and cyclization reactions, ARKIVOC i (2014) 307–336, doi:10.3998/ark. 5550190.0015.100.

[40] E.F. Ewies, M. El-Hussieny, N.F. El-Sayed, M.A. Fouad, Design, synthesis and bio-logical evaluation of novel αaminophosphonate oxadiazoles via optimized iron triflate catalyzed reaction as apoptotic inducers, Eur. J. Med. Chem. 180 (2019) 310–320, doi:10.1016/j.ejmech.2019.07.029.

[41] Y-H Wu, L-Y Zhang, N-X Wang, Y. Xing, Recent advances in the rare-earth metal triflates-catalyzed organic reactions, Catal. Rev. (2020) 1–37, doi:10.1080/01614940.2020.1831758.

[42] M.O. Sydnes, One-Pot Reactions: A Step Towards Greener Chemistry, Curr. Green. Chem. 1 (2014) 216–226, doi:10.2174/2213346101666140221225404.

[43] S.E. John, S. Gulati, N. Shankaraiah, Recent advances in multi-component reac-tions and their mechanistic insights: a triennium review, Org. Chem. Front. 8 (2021) 4237–4287, doi:10.1039/D0QO01480J.

[44] R.F. Barghash, W.M. Eldehna, M. Kovalova, V. Vojácková, V. Kryštof, H.A. Abdel-Aziz, One-pot three-component synthesis of novel pyrazolo[3,4-b]pyridines as potent antileukemic agents, Eur. J. Med. Chem. 227 (2022) 113952, doi:10.1016/j.ejmech.2021.113952.

[45] A. Kumar, Y. Kuang, Z. Liang, X. Sun, Microwave chemistry, recent advance-ments, and eco-friendly microwave-assisted synthesis of nanoarchitectures and their applications: a review, Materials Today Nano 11 (2020) 100076, doi:10. 1016/j.mtnano.2020.100076.

[46] P. Kafarski, M.G. Górniak, I. Andrasiak, Kabachnik-Fields Reaction under Green Conditions-A Critical Overview, Curr. Green Chem. 2 (2015) 218–222, doi:10.2174/2213346102666150109203606.

[47] S. Aita, V.N. Badavath, M. Gundluru, M. Sudileti, B.R. Nemallapudi, S. Gun-dala, G.V. Zyryanov, N.R. Chamarti, S.R. Cirandur, Novel α-Aminophosphonates

of imatinib Intermediate: Synthesis, Anticancer Activity, human Abl tyrosine kinase Inhibition, ADME and toxicity prediction, Bioorg. Chem. 109 (2021) 104718, doi:10.1016/j.bioorg.2021.104718.

[48] W.M. Abdou, M.S. Bekheit, One-pot three-component synthesis of pep-tidomimics for investigation of antibacterial and antineoplastic properties, Ar-bian J. Chem. 11 (2018) 1260–1269, doi:10.1016/j.arabjc.2015.04.014.

[49] W.M. Abdou, N.A. Ganoub, E. Sabry, Spiro- and substituted tetrahydrobenzo[b]thiophene-triazaphospholes and phosphoramidates as potent antineoplastic agents: Synthesis, biological evaluation, and SAR studies, Monatsh Chem 147 (2016) 619–626, doi:10.1007/s00706-015-1542-4.

[50] W.M. Abdou, N.A. Ganoub, E. Sabry, Synthesis of antimicrobial N-phthaloyl-alanyl-derived amidophosphates and triazoles, Naturforsch 64b (2009) 1057– 1064, doi:10.1515/znb-2009-0911.

[51] M.S. Bekheit, H.A. Mohamed, B.F. AbdelWahab, M.A. Fouad, Design and syn-thesis of new 1,4,5-trisubstituted triazole bearing benzenesulphonamide moi-ety as selective COX-2 inhibitors, Med. Chem. Research 30 (2021) 1125–1138, doi:10.1007/s00044-021-02716-7.

[52] I.A. Seliem, A.S. Girgis, Y. Motasim, A. Kandeil, A. Mostafa, M.A. Ali, M.S. Bekheit, S.S. Panda, New Pyrazine Conjugates: Synthesis, Computational Studies, and Antiviral Properties against SARS-CoV-2, Chem. Med. Chem. 16 (2021) 3418–3427, doi:10.1002/cmdc.202100476.

[53] S.I. Ali, A.A. Mohamed, M.Y. Sameh, O.M. Darwesh, T.M. Abd El-Razik, Gam-ma-Irradiation Affects Volatile Oil Constituents, Fatty Acid Composition and Antimicrobial Activity of Fennel (*Foeniculum vulgare*) Seeds Extract, Res. J. Pharm. Biol. Chem. Sci. 7 (2016) 524–532.

[54] O.M. Darwesh, K.M. Barakat, M.Z. Mattar, S.Z. Sabae, S.H. Hassan, Production of antimicrobial blue green pigment Pyocyanin by marine *Pseudomonas aerugi-nosa*, Biointerface Res. App. Chem. 9 (2019) 4334–4339, doi:10.33263/BRIAC95. 334339.

[55] Z.H. Kheiralla, M.A. Hewedy, H.R. Mohammed, O.M. Darwesh, Isolation of Pig-ment Producing Actinomycetes from Rhizosphere Soil and Application It in Textiles Dyeing, Res. J. Pharm. Biol. Chem. Sci. 7 (2016) 2128–2136.

[56] R.M. Abdelhameed, H.A. El-Sayed, M. El-Shahat, A.A. El-Sayed, O.M. Darwesh, Novel Triazolothiadiazole and Triazolothiadiazine Derivatives Containing Pyri-dine Moiety: Design, Synthesis, Bactericidal and Fungicidal Activities, Curr. Bioact. Compd 14 (2018) 169–179, doi:10.2174/1573407213666170127095158.

[57] O.M. Darwesh, I.E. Elshahawy, Silver nanoparticles inactivate sclerotial forma-tion in controlling white rot disease in onion and garlic caused by the soil borne fungus *Stromatinia cepivora*, Eur. J. Plant. Pathol. 160 (2021) 917–934, doi:10.1007/s10658-021-02296-7.

[58] P.A. Wayne, Methods for Dilution Antimicrobial Susceptibility Tests for Bacteria That Grow Aerobically, Approved Standard, CLSI document M07-A9, ninth ed., Clinical and Laboratory Standards Institute, 2012.

[59] J.H. Jorgensen, J.F. Hindler, L.B. Reller, M.P. Weinstein, New consensus guide-lines from the clinical and laboratory standards institute for antimicrobial sus-ceptibility testing of infrequently isolated or fastidious bacteria, Clin. Infect. Dis. 44 (2007) 280–286, doi:10.1086/510431.

[60] A.S. Kumar, J. Kudva, S.M. Kumar, U. Vishwanatha, V. Kumar, D. Naral, Synthe-sis, characterization, crystal structure, Hirshfeld interaction and bio-evaluation studies of 4-amino quinazoline sulphonamide derivatives, J. Mol. Structure. 1167 (2018) 142–153, doi:10.1016/j.molstruc.2018.04.055.

[61] A.S. Girgis, S.R. Tala, P.V. Oliferenko, A.A. Oliferenko, A.R. Katritzky, Computer-assisted rational design, synthesis, and bioassay of non-steroidal anti-inflammatory agents, Eur. J. Med. Chem. 50 (2012) 1–8, doi:10.1016/j.ejmech. 2011.11.034.

[62] A.S. Girgis, S.S. Panda, I.S.A. Farag, A.M. El-Shabiny, A.M. Moustafa, N.S.M. Is-mail, G.G. Pillai, C.S. Panda, C.D. Hall, A.R. Katritzky, Synthesis, and QSAR anal-ysis of anti-oncological active spiro-alkaloids, Org. Biomol. Chem. 13 (2015) 1741–1753, doi:10.1039/c4ob02149e.

[63] Z.M. Nofal, A.M. Srour, W.I. El-Eraky, D.O. Saleh, A.S. Girgis, Rational design, synthesis and QSAR study of vasorelaxant active 3-pyridinecarbonitriles incor-porating 1*H*-benzimidazol-2-yl function, Eur. J. Med. Chem. 63 (2013) 14–21, doi:10.1016/j.ejmech.2013.01.042.

[64] A.S. Girgis, S.S. Panda, M.N. Aziz, P.J. Steel, C.D. Hall, A.R. Katritzky, Rational de-sign, synthesis, and 2D-QSAR study of anti-oncological alkaloids against hep-atoma and cervical carcinoma, RSC Adv 5 (2015) 28554–28569, doi:10.1039/ C4RA16663A.

[65] http://www.codessa-pro.com/manuals/manual.htm

[66] https://www.chegg.com/learn/chemistry/inorganic-chemistry/coulombic-interaction